EFFECT OF FOAM DENSITY AND LOAD LEVELS ON FATIGUE CHARACTERISTICS OF PVC FOAM CORE SANDWICH COMPOSITES

Abdelhakim HADJAB [1,2], Louendi FATMI [3], Nouredine OUELAA [4]

The present study examines the mechanical, quasi-static, and cyclic fatigue characteristics of AIREX C70 PVC foam core sandwich composites featuring plain weave fiberglass/epoxy skins. The findings demonstrate that foam density and applied load levels profoundly influence the mechanical properties of these sandwich composites. Notably, following 10,000 cycles, the overall fatigue behavior parameters of AIREX C70.55 (60 kg/m^3) foam sandwiches exhibit a remarkable decrease of over 32%. In contrast, the corresponding values for AIREX C70.75 (80 kg/m^3) foam sandwiches display only a marginal variation of approximately 4%.

Keywords: sandwich structure, dissipated energy, fatigue, damage, foam density, load loss.

1. Introduction

Sandwich materials, which have a low-density core and high-strength skins, are popular in the aerospace and marine sectors due to their low weight and moisture resistance, but their fatigue behavior is a significant concern in dynamic load applications.

Zenkert and Burman [1] studied sandwich beam fatigue behavior, revealing a transition from core shear damage to laminate tensile fractures, and proposing a design scheme to account for these transitions.

Yang's [2] team examined the fatigue damage and static strength of sandwich structures using a polymethacrylimide foam core in three-point bending, comparing the results with a forecasting formula.

The authors [3] study uses flexural tests to establish the mechanical characteristics of sandwich composite materials, considering constructive, technological, and cost factors.

[1] Département de Génie Mécanique, Laboratoire de Mécanique et Structures (LMS), Université 8 mai 1945 Guelma, Algeria, email : hadjabh241065@gmail.com
[2] Département de Génie Mécanique, Université Echahid Cheikh Larbi Tébessi Tebessa, Algeria.
[3] Prof., Département de Génie Mécanique, Laboratoire de Mécanique et Structures (LMS), Université 8 mai 1945 Guelma, Algeria, e-mail : f_louendi@yahoo.fr
[4] Prof., Département de Génie Mécanique, Laboratoire de Mécanique et Structures (LMS), Université 8 mai 1945 Guelma, Algeria, e-mail : n_ouelaa@yahoo.fr

Wang et al [4] study investigates the fatigue behavior of composite sandwich beams made of GFRP skins, foam core, and additional stiffeners, focusing on failure modes, bending deflection, and fatigue life.

To prevent overestimating sandwich fatigue, A three-parameter fatigue design equation proposed by Dai and Liew [5] takes into account both the load range and the maximum applied load.

Mansouri et al. [6] note that fatigue tests exhibit a progression of stiffness degradation across cycles, characterized by three distinct phases. Sharaf et al. [7] observe that low cycle fatigue does not cause significant stiffness degradation, but results in residual deflections upon unloading, with greater deflections observed in 'soft' cores compared to 'hard' cores.

In [1], [8], and [9], The authors conducted a thorough investigation into the failure mechanisms of sandwich beams with PVC foam cores under static loading. Their findings revealed four distinct damage modes: core failure, face sheet debonding, compressive facing wrinkling, and indentation failure. According to microscopic investigations, the first damage is adhesive crack in the matrix/fiber, followed by core rupture [6]. Increasing the density of the foam core from 80 to 120 kg/m^3 does not significantly affect the bending strength characteristics of the sandwich panels [10]. Rupture modes identified in tested specimens consist of debonding between the core and skins, as well as cracks in the core at a 45° angle to the neutral axis of the sandwich [11]. While other studies evaluated fatigue damage to characterize residual stiffness or residual strength [12]–[14].

The purpose of this work is to understand the fatigue behavior of sandwich composites including foam cores through constant loading. This research contributes to gaining fundamental knowledge about the fatigue behavior of these materials and their response to constant loading conditions.

2. Materials and tests

This study uses AIREX C70.55 and C70.75 foam core sandwiches with densities of 60 and 80 kg/m^3, and woven composite laminate skins. The laminate consists of two layers of 2/2 twill woven glass fibers arranged in a $[0°/90°]_2$ stacking sequence and bonded together with epoxy resin. Sandwich beams will hereafter be referred to as H60 and H80, where the numerical value refers to the core density. These beams are cut from sandwich plates using a diamond disc. The study involved static skin characterization, static and fatigue testing of sandwich beams using a Zwick Roell Z005 testing machine with a 5 kN cell controlled by a computer, with the main properties of the foams outlined in Table 1, [15].

Table 1

Properties of AIREX C70 foam core[16]**.**

Properties	Norm	AIREX C70.55	AIREX C70.75
Density (kg/m^3)	ISO 845	60	80
Compressive modulus (MPa)	DIN 53421	59	83
Shear modulus (MPa)	ASTM C393	22	30

3. Static uniaxial tensile tests

To determine the elastic modulus, ultimate stress, and ultimate strain of the skins under study, uniaxial tensile tests were carried out on five specimens. The dimensions of the specimens are as follows: thickness (e) of 0.6 mm, width (b) of 15 mm, and length (L) of 250 mm. The distance between the grips used in the test is 138 mm.

The tests were conducted at a test speed of 2 mm/min, under room temperature conditions of 25ºC, following the guidelines specified in the ISO 527 [17] standard.

3.1 Result of tensile tests of skins

Young's modulus in longitudinal traction E_L is determined according to standard [17]. The traction module E_L is calculated between two stresses σ_1 and σ_2.

$$E_L = \frac{\sigma_2 - \sigma_1}{\varepsilon_2 - \varepsilon_1} \tag{1}$$

where:

σ_1 is the stress, measured at the strain value $\varepsilon_1 = 0.0005$,

σ_2 is the stress, measured at the strain value $\varepsilon_2 = 0.0025$.

The Young's modulus in transverse traction (E_T) is the same as the longitudinal modulus (E_L) because the quasi-static tensile mechanical properties of the 2/2 twill woven glass fibers are consistent in both directions. The test results are presented in Fig 1 and Table 2.

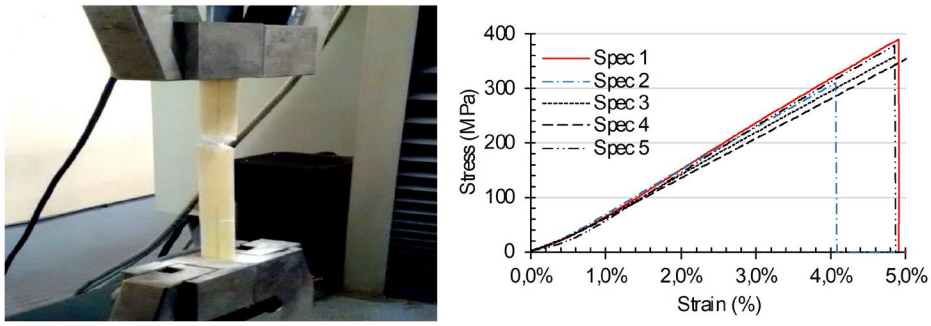

(a) (b)

Fig. 1. Mechanical behavior (a) and stress-strain curve (b) of the skins in static traction.

Table 2

Summary of tensile tests of the skins.

	specimens					averag e	Standard deviation
	1	2	3	4	5		
$E_L = E_T$ (GPa)	4,28	4,80	4,86	4,43	3,03	4,28	0,74
Ultimate stress (MPa)	388,89	308,88	356,67	372,22	377,78	360,89	31,30
Ultimate strain (%)	4,90	4,07	4,85	5,28	4,85	4,79	0,44

4. Three-point bending static test

These static tests were performed on H60 and H80 specimens, whose dimensions are displayed in Fig 2(b) and Table 3, using the "Zwick Roell Z005" machine (Fig. 2(a)). The test revealed that composite sandwich beam failure during the static three-point flexural test begins with compression fracture of the upper skin, and it is typically accompanied by delamination between the skin and the foam core.

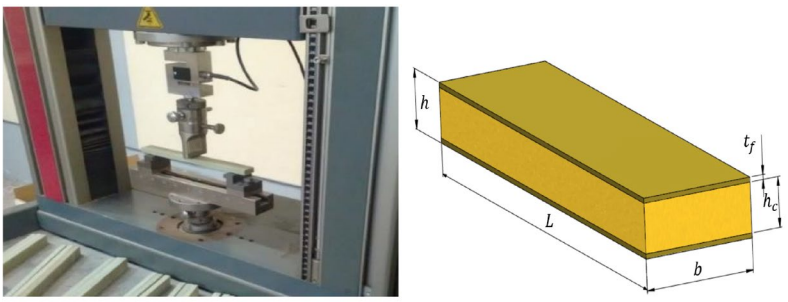

(a) (b)

Fig. 2. "Zwick Roell Z005" testing machine (a), Sandwich beam dimensions (b).

Table 3

The sandwich specimen's dimensions.

Specimen thickness h (mm)	Skin thickness t_f (mm)	Length of specimen L (mm)	Width of specimen b (mm)
10	0,6	200	20

4.1 Equivalent bending Young's modulus

Fig 3 shows the static three-point bending behavior of sandwiches H60 and H80, using four specimens and determining equivalent bending Young's modulus, E_{eq}, following ISO 178 standard, [18]. The modulus is determined by dividing the difference in stress values (σ_{f2} and σ_{f1}) by the difference in deformation ($\varepsilon_{f2} = 0.0025$ and $\sigma_{f2} = 0.0005$), with a 180 mm span between supports.

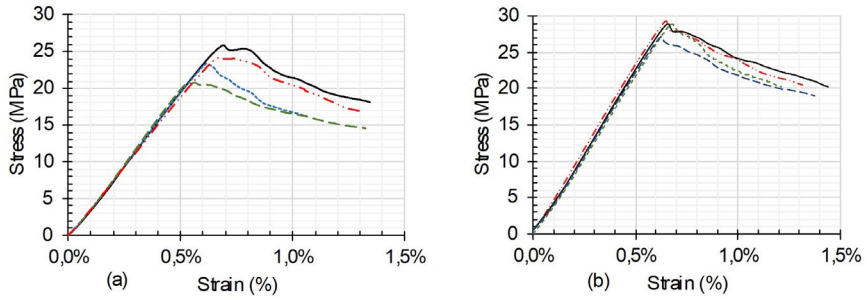

Fig. 3. Stress-strain three-point bending for composite sandwich beams: (a) H60, (b) H80.

$$E_{eq} = \frac{\sigma_{f2} - \sigma_{f1}}{\varepsilon_{f2} - \varepsilon_{f1}} \tag{2}$$

$$\varepsilon_{fi} = \frac{6h}{l^2} w_i \tag{3}$$

$$\sigma_{fi} = \frac{3l}{2bh^2} F_i \tag{4}$$

Where:

F_i: load applied by the pin (N)

l: the distance between supports (mm)

b: width of the specimen (mm)

h: thickness of specimen (mm)

w_i: displacement (mm)

ε_f: bending strain

σ_f: bending stress (MPa).

Table 4 displays the results of the three-point bending static test of the two studied sandwiches, including the equivalent Young's modulus E_{eq}, the ultimate flexural strength σ_{fu}, and the ultimate flexural strain ε_{fu}.

Table 4

Summary of bending tests for sandwich beams H60 and H80

		specimens				average	Standard deviation
		1	2	3	4		
H60	E_{eq} (GPa)	3,90	3,81	3,89	3,98	3,89	0,07
	σ_{fu} (MPa)	25,87	24,21	23,83	20,78	23,67	2,12
	ε_{fu} (%)	1,35%	1,30%	1,06%	1,33%	1,26%	0,13%
H80	E_{eq} (GPa)	4,661	4,326	4,291	4,245	4,381	0,19
	σ_{fu} (MPa)	29,30	28,94	27,15	28,87	28,56	0,96
	ε_{fu} (%)	0,65%	0,66%	0,63%	0,68%	0,65%	0,02%

5. Three-point bending fatigue test

Three-point bending fatigue tests, following the guidelines outlined in[19], were conducted on sandwich material beams H60 and H80. For fixture, two double-sided supports and a double-sided loading nose are used. The specimen is loaded or supported from the top by one side and the bottom by the other. The tests were carried out under various levels of stress (r) corresponding to 60%, 70%, and 80% of the static ultimate flexural strength (σ_{fu}) on a test bench equipped with a 5kN load cell. The beams were subjected to pulsed loads in the form of triangular waves, as illustrated in Fig 4(a), with a stress ratio (R) defined as the minimum applied stress ($\sigma_{f\min}$) to the maximum stress ($\sigma_{f\max}$) set to zero.

During the fatigue test, the beams were maintained at a constant displacement of 3 mm, and the bending speed was set at 45 mm/min. The sandwich beams were cycled at a frequency of 0.25 Hz. In a previous study [20], it was observed that when the bending load was set at 60% of the ultimate load and tested at frequencies of 1 Hz and 3 Hz, the specimens did not sustain complete damage. However, at the same bending load and a frequency of 9 Hz, the specimens failed due to delamination and core cracking.

The final cycle continued until failure occurred. Stress-strain curves were plotted for both sandwich materials, and the hysteresis cycles exhibited nearly elliptical curves, as depicted in Figs 4(b) and (c).

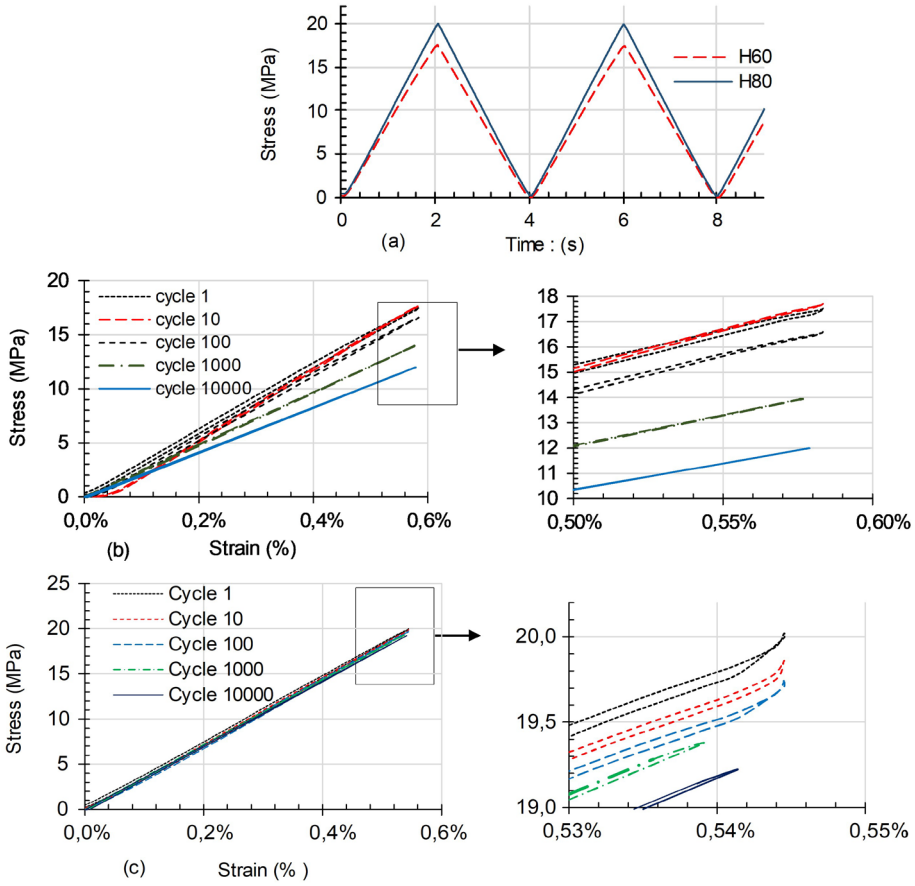

Fig. 4. Pulsed loads applied to sandwich beams (a) and hysteresis cycles corresponding to different numbers of cycles and at a loading level of 70%, for sandwiches: (b) H60, (c) H80.

5.1 Dissipated energy

The dissipated energy serves as a valuable metric for assessing the fatigue behavior of cellular foams. In a sandwich structure, the cellular foam core acts as an energy absorber, dissipating energy when subjected to impact or indentation.

In our study, specimens of sandwich material are subjected to cyclic fatigue through bending loading. As the load reaches a sufficient magnitude, it induces plastic deformation and damage, resulting in a hysteresis loop on the load-displacement curve, which represents the energy loss. The area enclosed by these curves signifies the energy dissipated during each cycle, while the area under the top (loading part) of the hysteresis loop corresponds to the maximum potential energy during the cycle. The numerical computation of the dissipated energy, E_d, is achieved by summing the areas using the trapezoid formula, as described in equation (5).

The area under the load-displacement hysteresis loops during loading represents the strain energy absorbed by the material. On the other hand, the area under the discharge curve represents the energy lost from the material. When the tested material is loaded beyond its elastic limit and enters the plasticity range, the absorbed energy exceeds the released energy, resulting in heat dissipation [21]. The dissipated energy is equivalent to the area enclosed by the hysteresis loop, as illustrated in Fig 5 (a).

$$E_d = \frac{1}{2}\sum_{1}^{n}(w_{i+1} - w_i)\left\{\left[L_{(w_{i+1})} + L_{(w_i)}\right] - \left[U_{(w_{i+1})} + U_{(w_i)}\right]\right\} \tag{5}$$

where:

E_d : dissipated energy,

$L_{(w_i)}$: load values at the top of the hysteresis loop (load) at displacement w_i,

$U_{(w_i)}$: load values at the bottom of the Hysteretic energy dissipation loop (unloading) at displacement w_i.

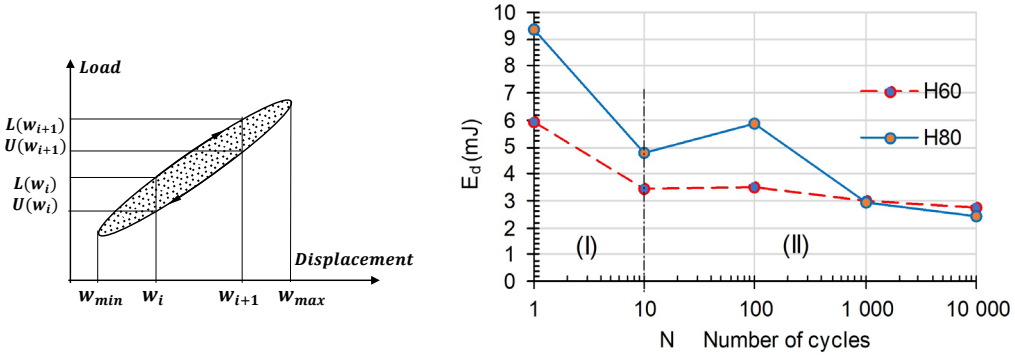

Fig. 5. Hysteretic energy dissipation (a) and the effect of the foam density on the dissipated energy (b).

The obtained results reveal the presence of two distinct phases, referred to as Phase I and Phase II, as illustrated in Fig 5 (b). Phase I, spanning from 1 to 10 cycles, is characterized by a sudden and linear decrease in dissipation. This decrease can be attributed to the formation of micro-cracks, followed by the rupture of the compressed matrix in the upper skin. Moving into Phase II, which encompasses 10 to 10,000 cycles, the dissipation of energy becomes significantly slower due to material degradation.

Furthermore, Fig 5 (b) presents the effect of foam density on the overall behavior of the material. The material with higher density exhibits a greater capacity for energy dissipation.

5.2 Equivalent Young's modulus in fatigue

The determination of the equivalent Young's modulus (E_{eq}) in flexural fatigue at a 70% loading level was carried out by the ISO 178 standard [18], considering various numbers of cycles. The results are shown in Fig 6, which displays the equivalent elasticity modulus evolution of the two studied sandwiches.

The results exhibit two distinct stages: an initial phase of linear elastic behavior observed within the first 100 cycles, followed by a rapid degradation from 100 to 10,000 cycles. Notably, the H60 sandwich experiences a more significant degradation compared to the other sandwich types during this stage.

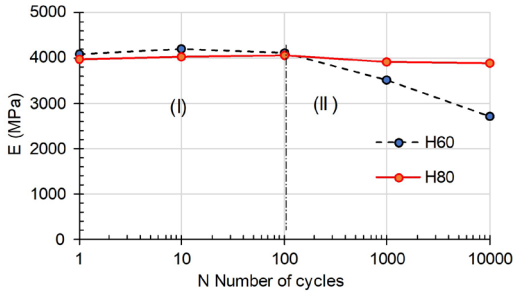

Fig.6. Foam density influence on the equivalent Young's modulus of the studied sandwiches at 70% loading level.

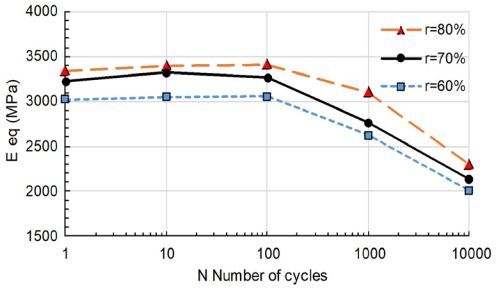

Fig. 7. Evolution of equivalent Young's modulus as a function of the number of cycles and different loading levels of sandwich H60.

The $E_{eq} - N$ graph, representing the growth of the equivalent Young's modulus, can be split into two zones. In the first zone ($N \leq 100$), the elastic modulus of both sandwiches remains constant. However, in the second zone ($N > 100$), the sandwich with lower foam density experiences a decrease in the equivalent modulus, ultimately leading to failure. This decrease can be attributed to the degradation of fiber strength, shearing interface, and foam crushing.

Furthermore, Fig 7 illustrates a noticeable decrease in the equivalent Young's modulus of the H60 material as the loading level decreases.

5.3 Relative load loss

In the fatigue test, we observe distinct stages of load loss $F_{max} / F_{max\,0}$ ($F_{max\,0}$ is the maximum load in the first cycle) in the H60 and H80 sandwiches until their rupture, as depicted in Fig. 8.

The first stage is characterized by an initial load reduction caused by cracking of the transverse layer and some early fiber fractures. The second stage is an intermediate period of stable fracture propagation during which load loss occurs as a result of increased matrix cracking, crack coupling at the layer interface, and initiation of internal delamination. The subsequent stage is characterized by a sharp decrease in load loss due to fiber breakage, which involves delamination and the combined effect of all degradation processes and ultimately leads to complete breakage of the laminate.

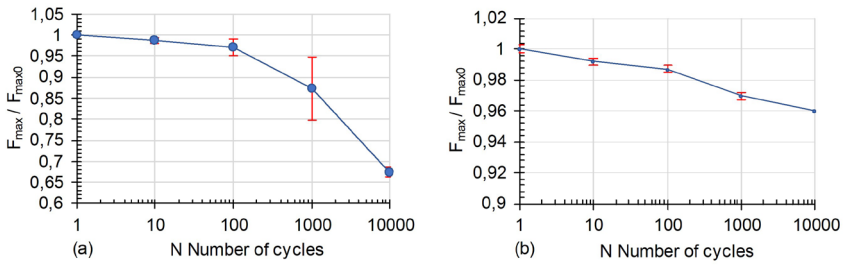

Fig. 8. Evolution of the load loss ($F_{max} / F_{max\,0}$) as a function of the number of cycles for a loading level of 70% and for sandwiches: a) H60, b) H80

6. Damage of sandwich

Images were captured and damage was measured using a binocular microscope (Visual Gage 250) equipped with software (Visual Gage 2.2.0), as shown in Fig.9 (a). The damage mode of the sandwich beams is illustrated in Fig.9 (b). The damage is represented in a 2D configuration, where fatigue damage was induced using a semi-cylindrical loading pin, as shown in Fig.9 (c).

During the fatigue test, it was observed that there was either no visible damage or minimal damage for the initial ten cycles. Subsequently, the level of damage in the sandwiches increased with higher loading levels and a greater number of cycles, as illustrated by Table 5. Notably, the material with the low-density foam exhibited more pronounced damage compared to the others.

Micro-cracks initially form during the early stages of the fracture process and gradually evolve into larger cracks, as shown in Table 5.

Before the failure of the specimens, three distinct events were observed:

1. The first event leads to the indentation of the compressed skin.

2. Subsequently, this indentation causes crushing of the sandwich core foaming, leading to the failure of the compressed skin.

3. The third event involves the shearing of the foam, propagating towards the second skin.

It should be noted that H60 sandwich beams are more susceptible to crushing damage than H80 sandwich beams. In both types of sandwiches, the main form of damage is fiber breakage, while core crushing occurs specifically in H60 sandwich beams.

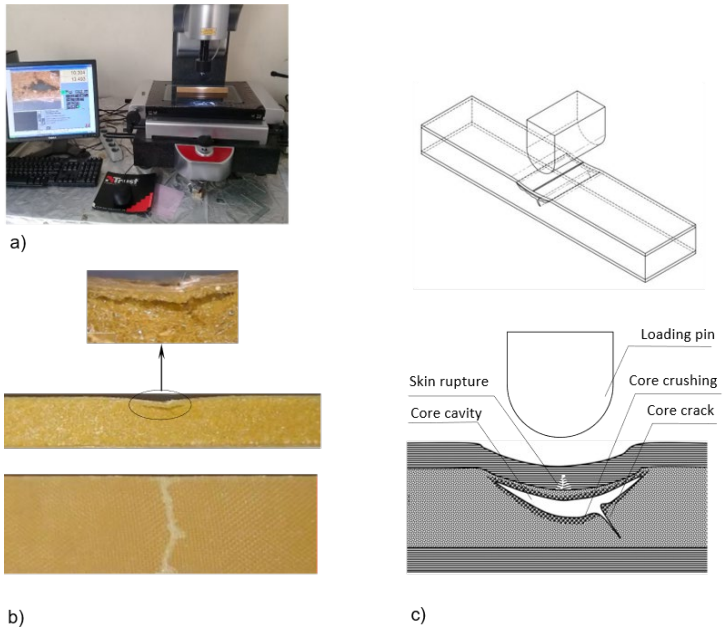

Fig. 9. The binocular microscope (a), macroscopic and microscopic observations (b), scheme (c) of the damage mode of sandwich panels.

Table le 5

Evolution of composite sandwich damage as a function of the number of cycles and for different loading levels

Cycles		100	1000	10000
		H80		
Loading levels	60%	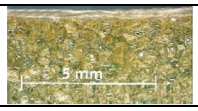	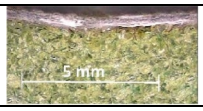	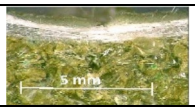

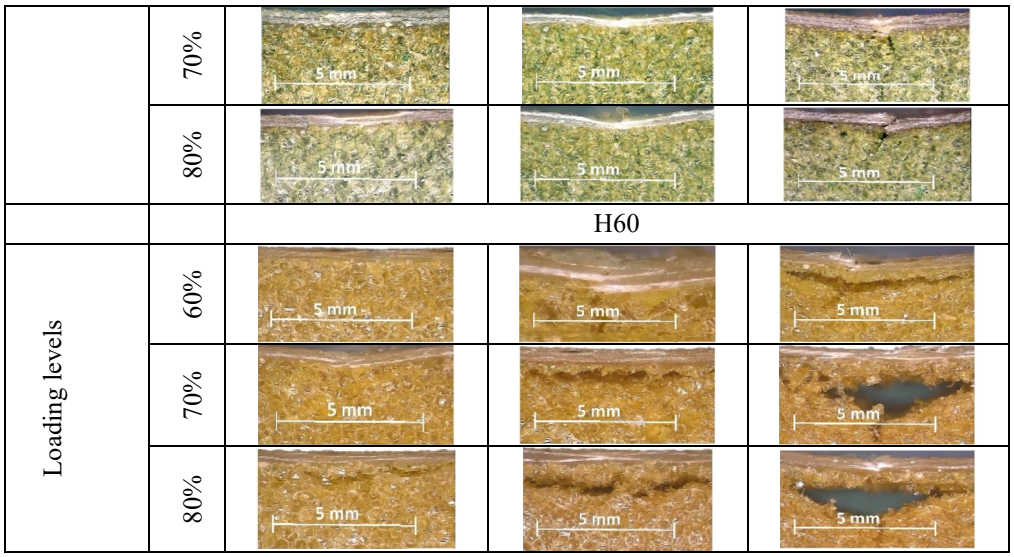

Conclusions

In this study, the fatigue behavior of sandwich materials under three-point bending with foams of different densities is analyzed. The obtained data indicate that the level of loading and the density of the foams have a significant impact on the fatigue behavior of the sandwiches. The global parameters studied include the equivalent of Young's modulus in bending, load loss, and energy dissipation.

For foam sandwiches with a density of 60 kg/m^3, the load loss and equivalent Young's modulus decreased by 32% after 10,000 cycles. In contrast, samples with a density of 80 kg/m^3 exhibited a small variation of approximately 4%.

Additionally, two distinct zones were observed, corresponding to different cycling levels (I and II). The first zone (1-100 cycles) demonstrated a linear decrease in energy dissipation, attributed to the formation of micro-cracks. The second zone (100-10,000 cycles) exhibited a rapid decrease in energy dissipation due to material degradation. The observed increase in damage aligns well with the calculated parameters ($E, E_d, F_{\max} / F_{\max 0}$) of the studied materials, thus justifying the evolution of damage in the sandwich beams.

REFERENCES

[1]. *M. Burman and D. Zenkert*, "Fatigue of foam core sandwich beams - 1: Undamaged specimens," Int. J. Fatigue, **vol. 19**, no. 7, pp. 551–561, 1997,.

[2]. *F. P. Yang, Q. Y. Lin, and J. J. Jiang*, "Experimental study on fatigue failure and damage of sandwich structure with PMI foam core," Fatigue Fract. Eng. Mater. Struct., **vol. 38**, no. 4, pp. 456–465, 2015,.

[3]. *M. L. Scutaru, C. Itu, M. Marin, and H. S. Grif*, "Bending Tests Used to Determine the

Mechanical Properties of the Components of a Composite Sandwich Used in Civil Engineering," Procedia Manuf., **vol. 32**, pp. 259–267, 2019, available: https://doi.org/10.1016/j.promfg.2019.02.212.

[4]. *B. Wang, Y. Shi, C. Zhou, and T. Li*, "Failure mechanism of PMI foam core sandwich beam in bending," Int. J. Simul. Multidiscip. Des. Optim., **vol. 6**, p. A8, 2015,.

[5]. *X. X. Dai and J. Y. Richard Liew*, "Fatigue performance of lightweight steel-concrete-steel sandwich systems," J. Constr. Steel Res., **vol. 66**, no. 2, pp. 256–276, 2010, available: http://dx.doi.org/10.1016/j.jcsr.2009.07.009.

[6]. *L. Mansouri, A. Djebbar, S. Khatir, H. T. Ali, A. Behtani, and M. A. Wahab*, "Static and fatigue behaviors of short glass fiber–reinforced polypropylene composites aged in a wet environment," J. Compos. Mater., **vol. 53**, no. 25, pp. 3629–3647, 2019,.

[7]. *T. Sharaf, W. Shawkat, and A. Fam*, "Structural performance of sandwich wall panels with different foam core densities in one-way bending," J. Compos. Mater., **vol. 44**, no. 19, pp. 2249–2263, 2010,.

[8]. *C. A. Steeves and N. A. Fleck*, "Collapse mechanisms of sandwich beams with composite faces and a foam core, loaded in three-point bending. Part I: Analytical models and minimum weight design," Int. J. Mech. Sci., **vol. 46**, no. 4, pp. 561–583, 2004,.

[9]. "Collapse mechanisms of sandwich beams with composite faces and a foam core, loaded in three-point bending. Part II: Experimental investigation and numerical modelling," Int. J. Mech. Sci., **vol. 46**, no. 4, pp. 585–608, 2004,.

[10]. *A. Shalbafan, J. Luedtke, J. Welling, and A. Fruehwald*, "Physiomechanical properties of ultra-lightweight foam core particleboard: Different core densities," Holzforschung, **vol. 67**, no. 2, pp. 169–175, 2013,.

[11]. *K. Bey, K. Tadjine, R. Khelif, A. Chemami, M. Benamira, and Z. Azari*, "Mechanical Behavior of Sandwich Composites Under Three-Point Bending Fatigue," Mech. Compos. Mater., **vol. 50**, no. 6, pp. 747–756, 2015,.

[12]. *J. Dai and H. . Hahn*, "Fatigue Analysis of Sandwich Beams Using a Wear-out Model," **vol. 38**, no. 7, pp. 581–589, 2003,.

[13]. *G. . Sendeckyj*, "Life Prediction for Resin-matrix Composite Materials," Fatigue Compos. Mater., **vol. 4**, pp. 431–480, 1990,.

[14]. *A. El Mahi, M. Khawar Farooq, S. Sahraoui, and A. Bezazi*, "Modelling the flexural behaviour of sandwich composite materials under cyclic fatigue," Mater. Des., **vol. 25**, no. 3, pp. 199–208, 2004,.

[15]. *J. P. M. Cheloni, M. E. Silveira, and L. J. Da Silva*, "Effects of amount of glass fiber laminate skins in sandwich composite of filled core," Mater. Res., **vol. 22**, no. 1, pp. 1–8, 2018,.

[16]. *3A Composites Core Materials*, "AIREX ® C70," 2020. available: https://www.3accorematerials.com/uploads/documents/TDS-AIREX-C70-E-04.2020.pdf. [Accessed: Dec. 06, 2020].

[17]. *ISO 527-5:2009*, "Determination of tensile properties - Part 5: Test conditions for unidirectional fibre-reinforced plastic composites," Int. Organ. Stand., **vol. 1**, p. 9 pp., 2009.

[18]. *BS EN ISO 178:2003*, "Plastics—Determination of flexural properties, EN ISO 178: 2003," **vol. 3**, p. 28, 2003.

[19]. *D 7774*, "Standard Test Method for Flexural Fatigue Properties of Plastics 1," **vol. i**, pp. 1–7, 2017,.

[20]. *B. J. Manujesh and V. Rao*, "Fatigue Behavior and Failure Mechanism of PU Foam Core E-

glass Reinforced Vinyl Ester Sandwich Composites," Int. J. Mater. Eng., **vol. 3**, no. 4, pp. 66–81, 2013,.

[21]. *K. Kanny and H. Mahfuz*, "Flexural fatigue characteristics of sandwich structures at different loading frequencies," Compos. Struct., **vol. 67**, no. 4, pp. 403–410, 2005,.